

# Active Aerodynamic Control of Wake-Airfoil Interaction Noise—Experiment

J. Simonich\* and P. Lavrich†

*United Technologies Research Center, East Hartford, Connecticut 06108*

and

T. Sofrin‡ and D. Topol§

*Pratt & Whitney Aircraft, East Hartford, Connecticut 06108*

A proof of concept experiment has been performed that shows the potential for active aerodynamic control of rotor wake/stator interaction noise in a simplified manner. A single airfoil model representing the stator was fitted with a movable trailing-edge flap controlled by a servomotor. This flap allowed control of the unsteady lift of the airfoil and acted as the active aerodynamic element in the system. Upstream of the airfoil, a disturbance generator created a periodic wake, similar to an actual rotor blade wake, which impinged on the airfoil. A control system moved the motor-driven flap in the correct angular displacement rate and phase to reduce the unsteady load on the airfoil during the wake interaction. The motion could be arbitrary, permitting the airfoil-flap combination to respond to generic inflow disturbances. Noise reduction results showed that this concept works very well in the bandwidth at which the servomotor drive actuated the flap (currently up to 100 Hz). The peak-to-peak acoustic interaction pulse was reduced by a factor of 2, whereas the corresponding noise was reduced by a significant 10 dB at some frequencies. A companion paper by E. J. Kerschen, entitled "Active Aerodynamic Control of Wake-Airfoil Interaction Noise—Theory," demonstrates the ability to predict the required flap motion to achieve these dramatic noise reductions.

## Introduction

### Interaction Noise Mechanisms

A N important source of unsteady lift, vibration, and noise in rotating machinery occurs when asymmetric inflows are convected into a rotor. Similar effects occur when convected wakes or gusts (from an upstream rotor or vane) impinge on a downstream rotor or stator. These phenomena are known as gust/airfoil interaction, wake cutting, or blade wake interaction. The unsteady forces on the airfoil create mechanical vibration, whereas the unsteady surface pressure field generates a dipole type of noise radiation.<sup>1,2</sup>

Rotor/stator interaction noise is influenced by the gap spacing between the rotor and the stator. Except for very close spacings, the potential field influence is much smaller than the effect of viscous wake/flow interactions. The wake shape also has an influence on the intensity of the various acoustic harmonics.<sup>3,4</sup>

Fujita and Kovaszny<sup>5,6</sup> conducted an experiment to study the transient response of an isolated airfoil to a passing wake generated by a cylindrical rod. Both unsteady surface pressures and far-field acoustic data were obtained. The sound radiation in the direction normal to the airfoil was found to be purely dipole in character. Two-dimensional wake interactions (airfoil leading edge aligned with the wake) and skewed wake interactions were studied. Both the pressure fluctuations and the noise were found to decrease with increasing skew angle between the airfoil and the wake. These tests were extended to

a linear cascade by Ho and Kovaszny<sup>7</sup> in 1975. They noted a significant difference in transient response depending on the direction of the passage of the wakes, i.e., whether the suction or the pressure surface of the cascade vane was struck first.

A similar study conducted by Sugeng and Fiedler<sup>8</sup> used a cascade of highly cambered stator vanes and a cylindrical rod rotor. They showed wake defects of 20% and peak-to-peak variations of angle of attack of +5 to -8 deg. Increasing the rotation speed increased the unsteady blade force fluctuations, whereas increasing the axial velocity had only a small effect.

An experimental study of the turbofan interaction noise generation mechanism was performed by Zandbergen<sup>9</sup> in 1988. He studied the effect of wakes from both cylindrical rods as well as a lightly loaded rotor impinging on an annular cascade of vanes. Unsteady radial velocity fluctuations measured by a hot wire showed variations in flow angle up to 8 deg at the hub. Unsteady pressure differences were at a maximum near the leading edge and were dominated by blade passing frequency. Downstream from the leading edge, however, higher harmonics may become important. Peak unsteady lift coefficients occurred when the leading edge of the vane was near the wake centerline.

Several techniques can be used to reduce interaction noise. One technique is to increase the spacing between the rotor and the stator so that the sharpness of the wake deficit is smoothed out. Another option for engine designers is to add noise attenuation treatment in the nacelle. Both of these techniques add undesirable size and weight to the engine and the total practically achievable noise reduction is limited to a few decibels. Although using active aerodynamic control to reduce interaction noise adds complexity, it offers the potential for a breakthrough noise reduction of 10–20 dB.

### Background/Motivation

Active control is a term used to describe techniques that monitor some parameter of system performance and apply corrections to compensate for changing operating conditions. Intelligent controllers acquire data from sensors and decide on a course of action to bring some phenomena within specifications. With the availability of inexpensive and powerful mi-

Presented as Paper DGLR/AIAA 92-02-038 at the DGLR/AIAA 14th Aeroacoustics Conference, Aachen, Germany, May 11–14, 1992; received Oct. 14, 1992; revision received Feb. 5, 1993; accepted for publication Feb. 9, 1993. Copyright © 1993 by United Technologies Corporation. Published by the American Institute of Aeronautics and Astronautics, Inc., with permission.

\*Senior Research Engineer, Aeroacoustics and Experimental Gas Dynamics, MS 129-17, 411 Silver Lane. Senior Member AIAA.

†Senior Research Engineer, Aeroacoustics and Experimental Gas Dynamics, MS 129-17, 411 Silver Lane. Member AIAA.

‡Engineering Consultant, 400 Main Street.

§Senior Engineer, Acoustics Engineering, MS 123, 400 Main Street. Member AIAA.

croprocessors, active control has recently been applied to a wide variety of different disciplines, including acoustics, combustion, gas turbine system stability, and flow control. Several commercial products have already been introduced in the noise reduction area, including electronic automobile mufflers, actively controlled headphones, and quiet refrigerators.

Noise cancellation by active control is simple in concept, although not in practice. The sound from an unwanted source can be canceled by introducing sound that is equal in amplitude but out of phase by 180 deg. This antisound or antinoise concept has been known for some time. The idea was patented by Lueg in 1936,<sup>10</sup> but interest and practical applications of antinoise did not appear until the 1970s and 1980s when the appearance of inexpensive, powerful digital signal processing microchips made the concept viable. There are several excellent reviews of active noise control that discuss the state of the art.<sup>11,12</sup> Applications of the technique are as varied as the use of sound to control flow separation,<sup>13</sup> propeller noise control,<sup>14-16</sup> cancellation of blade harmonics in centrifugal fans,<sup>17</sup> interior noise reduction in aircraft cabins,<sup>18,19</sup> and reduction of blade-vortex interaction noise in helicopter rotors.<sup>20</sup>

In practice, the application of the antisound approach has some limitations. Since the unwanted sound must be canceled by spatially discrete sources (speakers) that are usually placed some distance from the noise source, it is not always possible to have a global noise reduction over all space. This means that some regions will experience a noise reduction whereas others exhibit a noise increase. The concept has been commercially applied only in simple geometries such as one-dimensional ducts where the acoustic field is a simple wave. The antisound technique has also been limited to low frequencies since the method relies on sampling the noise and processing it for a short time before introducing the canceling sound field. By locating the canceling speaker upstream of the sensing station, a processing time of several milliseconds is available. At higher frequencies, the microprocessor speed becomes a limitation. In addition, introducing antisound can require very large and powerful amplifiers and loudspeakers. In any case, the sound source is unaltered.

The concept we have demonstrated is fundamentally different in that it attacks the offending noise at the source of the sound. Rotor/stator interaction noise is caused by vane surface pressure fluctuations that are set up by changes in flow incidence angle caused by the wake of an upstream rotor. The instantaneous lift on the airfoil changes during the wake encounter. The concept for aerodynamic active control is to reduce or eliminate the unsteady lift during a rotor wake/vane interaction, thereby reducing the interaction noise. This eliminates the noise at the source and is therefore an inherently global noise reduction technique.

### Objectives

The application of active control investigated in this joint Pratt and Whitney/United Technologies Research Center (UTRC) program was directed at assessing the use of active aerodynamics to reduce high bypass ratio aircraft engine noise. Fan noise from such engines is dominated by interaction tones that are caused by airflow disturbances, generated by fan wakes, impinging on a downstream stator row. This interaction causes a fluctuating lift on the following stator blade row and leads to noise. Currently, the gap spacing between rotor and stator rows is partially dictated by the noise generated by this mechanism. An increase in noise occurs as the spacing is decreased. The overall goal of the current program was to find techniques for reducing the interaction noise, thereby allowing the rotor/stator gap to be reduced. A gap reduction would result in shorter and hence lighter engines.

### Approach

One approach to reducing the strength of the gust/airfoil interaction is to suppress spatially nonuniform inflows. A second approach is to increase the axial spacing between rotor-stator components so that the wake velocity gradients smooth

out and decay before they impinge on the stator. Unfortunately, these strategies are not always practical.

The technique proposed here to reduce the gust/airfoil interaction unsteady loading is to apply active aerodynamic control. In the present two-dimensional simulation study, the fixed stator component is replaced by a two-dimensional vane in a rectangular duct subject to a periodic incident gust. The gust interaction is countered by introducing unsteady lift on the vane using an oscillating trailing-edge flap.

### Interaction Facility

The rotor/stator interaction facility was designed as a simulation facility to investigate the aeroacoustic phenomenon related to the unsteady aerodynamics of fan rotor and stator interactions. A schematic and a photograph of the facility are shown in Figs. 1 and 2. A low-noise environment is provided for acoustic measurements. The facility is of open circuit design; however, the flow is recirculated in the laboratory to maintain reasonably constant flow properties. Flow is produced by a rooftop-mounted blower that is acoustically treated with low-pressure-loss mufflers on both the blower inlet and outlet. A freestream flow rate of 125 ft/s is provided through the 24-in. high by 6-in. wide (stator spanwise direction) test section.

A unique characteristic of the facility is the 6-ft-diam gust generator that is located just downstream of the 6:1 flow contraction. Two tapered cylindrical rods rotate through the tunnel flow driven by a variable speed dc motor capable of tip speeds from 0 to 125 ft/s. These rods generate wakes or gusts that convect through the test section to the downstream airfoil. The rods sweep through the test section from below the airfoil to above.

The vane consisted of a 6-in. chord, 6-in. span symmetric NACA 0009 airfoil, providing a relatively thin profile shape with well-established aerodynamic section properties. The vane leading edge was typically located 3 in. downstream of

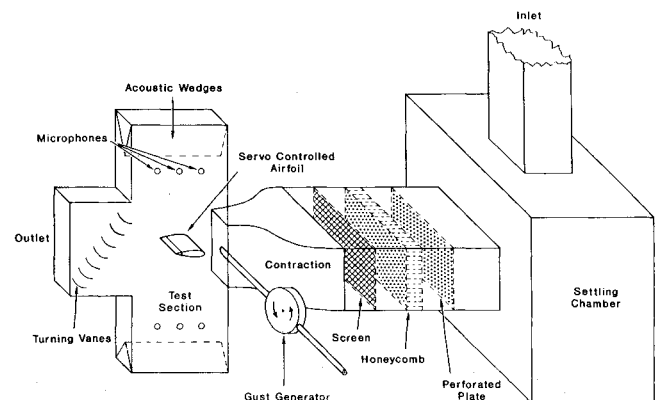


Fig. 1 Schematic diagram of rotor/stator interaction facility.

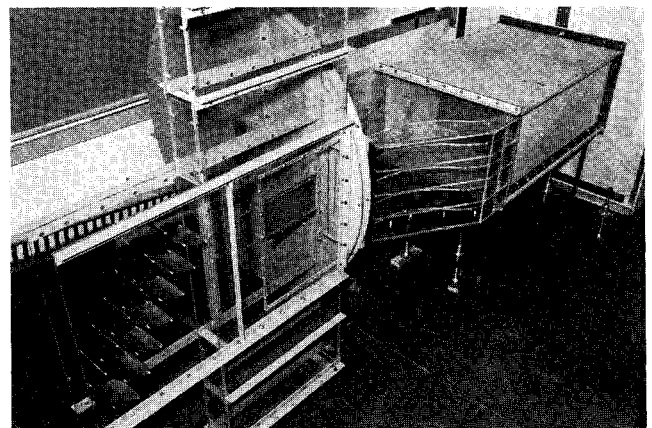


Fig. 2 Photograph of rotor/stator interaction facility.

the center of the gust generator rotation plane. The aft 20% of the airfoil was hinged to provide a trailing-edge flap with a direct drive servomotor and rotary encoder. Operating characteristics of the flap provide  $\pm 10$  deg of motion with at least a 100-Hz frequency response.

### Simulation

Fan rotor/stator interaction noise reduction by active noise control in an actual gas turbine engine will be a challenge. In an actual turbomachine, the interactions occur at high speed, resulting in high acoustic frequencies. In terms of acoustic reduced frequency defined by Amiet,<sup>21</sup>

$$\mu = \frac{n\omega b}{c(1 - M^2)} \quad (1)$$

where  $n$  is the number of blades,  $\omega$  is the circular frequency (rad/s),  $b$  is the vane semichord,  $c$  is the speed of sound, and  $M$  is the inflow Mach number. The range of values for a modern turbofan range from  $\mu = 0.8$ – $3.0$ . The engine also contains multiple rotor blades and stators in an annular cascade that gives rise to swirling modes and duct propagation with cuton and cutoff frequencies. The noise source mechanism is also noncompact.

To simplify the engine problem to more tractable geometry and operating conditions, thereby allowing an investigation of the current control concept, a simulation study was performed. The stator cascade was represented by an isolated airfoil. For the airflow velocities of the interaction rig (125 ft/s), the rotor speed was selected at 300 rpm, yielding a blade passage, acoustic reduced frequency of  $\mu = 0.014$ . For this frequency, the noise source is compact, since the general criterion for compactness is  $\mu^2 \ll 1$ .

In the actual engine where the source of the blade passage frequency is noncompact, each point of the surface radiates sound independently. Planar surfaces can produce strong beaming. Any antisound approach must match the details of the source characteristics. In comparison, the technique investigated here is valid only with compact noise sources, which respond to changes in unsteady vane lift. This limited simulation is justified since the objective of the study was to determine the feasibility of active control for rotor/stator interaction noise reduction. A successful demonstration of the active aerodynamic control concept in the compact domain provided confidence that the technique might also succeed in the more difficult noncompact case. The purpose of the current study was not to design hardware that could be installed in an engine but instead to conceive advanced concepts that could. The study succeeded in this respect by providing valuable insight into active control concepts, actuation methods, control hardware, and algorithms for interaction noise reduction. The program also provided a foundation for development of more advanced applications of active control in the noncompact domain.

### Experimental Layout

The basic layout of the experiment was modeled after the successful experiment of Fujita and Kovaszny.<sup>5,6</sup> Several items were improved. A two-dimensional duct was chosen instead of an open jet to provide a uniform vane lift across the span without tip effects. A two-dimensional duct also yields two-dimensional acoustic wave spreading at  $1/\sqrt{r}$  instead of  $1/r$  for spherical spreading, thereby producing a stronger wave front. The gust generator rods were tapered to produce a uniform velocity defect across the span.

### Actuated Airfoil

A schematic diagram of the actuated trailing-edge flap motion control system is shown in Fig. 3. This concept was chosen over other control techniques such as pistons or jet flaps since it was simple to implement and well understood. Likewise, a servomotor was chosen to move the flap since it

was a readily available, inexpensive commercial technology. A trailing-edge flap was chosen over a leading-edge flap since a preliminary study by Kerschen<sup>22</sup> determined that for low values of aerodynamic reduced frequency  $k = \omega b/U$ , trailing-edge flaps were found to be much more effective than leading-edge flaps. (At higher reduced frequencies, the effectiveness of leading-edge flaps approaches that of trailing-edge flaps.)

An NACA 0009 symmetric airfoil shape was chosen for the vane since it is relatively thin, similar to modern fan blades, and has well-established aerodynamic properties. The 20% chord trailing-edge flap was made of aluminum and the interior was hollow to reduce its inertia.

### Servomotor Control

Servomotor motion control was provided by a general purpose motion control interface card for a personal computer. Programming functions were provided to the card through the PC using Fortran calls to assembly language routines to directly load and read registers in the motion control interface card. The actual position achieved by the motor was returned from an incremental position encoder.

### Acoustic Measurement Technique—Net Dipole

Acoustic data were obtained by two microphones mounted in the test section, one 40 in. directly above and one below the actuated vane. Half-inch diameter microphones were chosen because of their low frequency response and high output characteristics. The microphone locations were selected because the gust interaction is known to be dipole in character and directivity lobes were expected to peak in this orientation. The microphone signals were fed into a dual-channel dynamic signal analyzer. The digital data were transferred to the laboratory computer via the IEEE-488 interface on both devices.

### Slant Hot Wire

Velocity measurements of the wakes from the gust generator rods were acquired to document the structure of the gusts incident on the vane and to check for two-dimensionality of the flow. All velocity measurements were acquired with a single-slanted sensor hot-wire technique. This technique uses a single sensor, rotated about its axis to at least three orientations, to discern the complete three-component velocity vector. The basic elements of this technique will be summarized here but are found in more detail in Lavrich.<sup>23</sup> This technique provides an aerodynamically clean, compact, and relatively simple method to measure the three components of mean velocity in stationary or periodic flows.

At least three separate measurements are acquired by rotation of the probe about its axis. This rotation changes the yaw angle in known increments. If the directional sensitivity of the sensor is known, a set of three equations can be solved for the three unknown velocity components. Three measurements are sufficient to unambiguously determine the three unknowns (velocity magnitude and the two flow angles). However, data

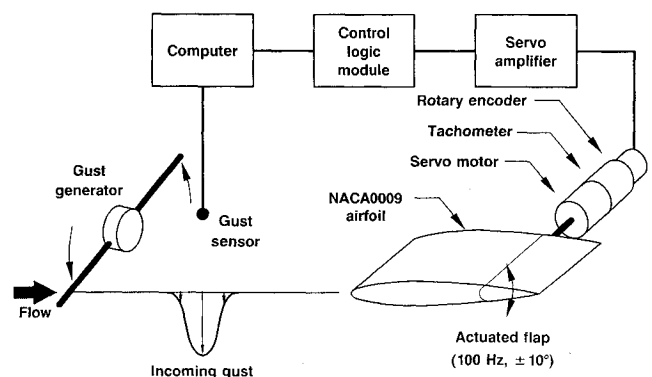


Fig. 3 Schematic diagram of actuated trailing-edge flap control.

from additional orientations can be used with a least-squares optimization to reduce sensitivity to signal noise.

This flow measurement technique yields effectively the same information (at least for mean velocity) as a triple sensor probe, without three individual sensors and electronics. The directional sensitivity of the wire used during this experiment was directly calibrated in a computer-controlled, calibration facility that allowed relatively simple, accurate, and repeatable calibrations of the wire to be performed. Direct calibration eliminates uncertainties in directional response using theoretical expressions.

Since the flow at a given point is measured by the slanted hot wire at several different times (corresponding to time required to rotate the wire to different orientation angles), some averaging of the wire signal must be performed to assure that the same flow is seen by the hot-wire sensor. For this application, the hot-wire voltage was ensemble averaged phase locked to a 1/rev signal of the gust generator. This averaging preserved the rod-to-rod flow character of the signal, while suppressing the random components (any signal not locked to 1/rev such as turbulence). Accuracy of the technique is limited to about  $\pm 5\%$  of the total velocity and to  $\pm 2$  deg of angle (both pitch and yaw angles).

The nonlinearized hot wire was digitally sampled at 5689 Hz and antialias filtered at 2 kHz. This sampling rate enabled 1024 points to be acquired in 90% of a revolution. A 100-record ensemble average was acquired. Surveys were obtained at 0.5-in. increments across the span at the quarter-chord location of the vane to check the two-dimensionality of the gust wake. (The vane was removed during these measurements.)

#### Surface Pressure

For a compact source, the interaction noise is directly related to the instantaneous lift on the vane. The instantaneous lift is a result of the instantaneous surface pressure acting on the vane. To measure the chordwise distribution of unsteady surface pressures on the vane, a 1/8th-in. microphone was flush mounted on the sidewall of the test section along the upper airfoil surface/endwall junction. Gust-synchronized, ensemble-averaged measurements were obtained at seven stations along the vane chord. Data were obtained for the baseline, unactuated case only.

It should be pointed out that the flowfield in the vicinity of the airfoil/sidewall junction is non-two-dimensional, due to the junction horseshoe vortex. However, the static pressure on the airfoil is composed of two parts: a mean component and an unsteady component. Although the junction flow will influence the mean static pressure distribution along the chord at the endwall, the unsteady pressure should not be affected to the same extent.

To qualify the measurement of unsteady surface pressure at the sidewall/airfoil junction as representative of the unsteady static pressure on the airfoil at midchord, a single high-response pressure transducer was mounted at the midspan of the airfoil at 10% chord. Its signal was compared with the sidewall microphone signal at the same chordwise station. The two signals agreed very well, thereby confirming that the sidewall measurement technique works for this application with synchronous averaging of a periodic signal.

#### Control Strategy

In typical antinoise active control strategies, an electronic controller is used to sense and minimize an undesirable noise. In principle, this "black box" technique adjusts the parameters it controls and determines the appropriate response to take for each input condition. In practice, sophisticated algorithms are used to determine a response that will minimize the noise.

The current approach was simpler in concept. The rotor/stator interaction is a primarily periodic event with randomness superimposed on the aerodynamic and acoustic responses due to turbulence or vortex shedding. Because of the periodic

nature of the interaction process, it was not necessary to have a controller that could sense and respond to individual gusts. Instead, the flap motion was programmed to respond to the ensemble-averaged gust for each and every gust. The function that was minimized in this process was the net dipole interaction noise. The controller was open loop in the sense that the test operator controlled the shape and phase of the flap motion. This motion and any delay time were manually chosen to minimize the noise based on intuition and engineering judgment.

## Results

#### Synchronized Wake Profiles

Three-dimensional, ensemble-averaged, synchronized velocity measurements were made of the wakes downstream of the gust generator rods to measure the driving function for the interaction noise and to check for two-dimensionality of the flow. This input is needed for any theoretical analysis of gust response. These measurements describe the gust generator velocity perturbation that is incident on the vane and is conse-

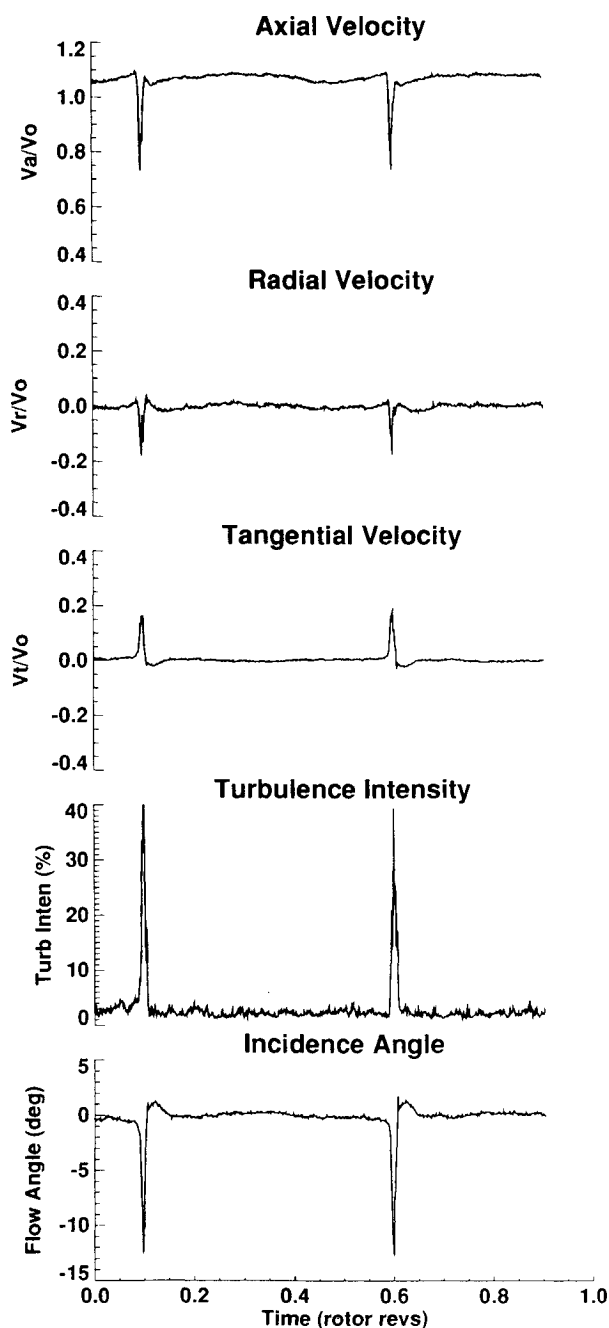


Fig. 4 Gust-synchronized velocity measurements at airfoil location.

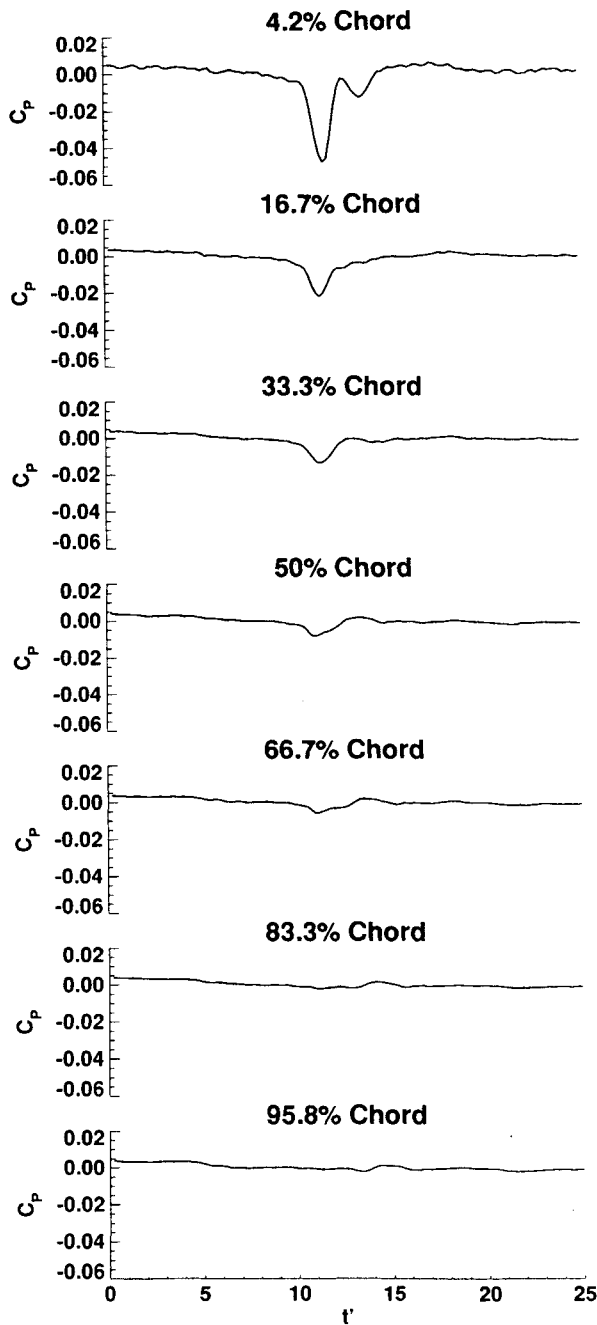


Fig. 5 Gust-synchronized surface pressure for unactuated flap.

quently responsible for the surface pressure disturbance and hence the noise.

The results for the midspan location are shown in Fig. 4. Five plots are shown: the three velocity components normalized by the freestream velocity, the turbulence intensity, and the incidence angle. Hence, the radial direction is defined as positive outward from the gust generator hub. The tangential velocity is positive in the direction of rod rotation (counterclockwise as viewed from downstream and vertically upward through the test section). The incidence angle is computed by using the axial and tangential velocities only. It represents the flow incidence angle that a two-dimensional gust would make with a two-dimensional vane.

For the central portion of the test section span (data between  $X = 1.5$  and  $4.5$  in. or 25–75% span), the flow appears uniform and two dimensional. A high degree of periodicity is provided by the two rods since rod-to-rod differences were small. Since there were only two rods, the interaction between the rod wakes was negligible. There is an axial wake defect

associated with the rods with a value of 30% of the freestream. The radial and tangential velocity component changes caused by the rod wakes are similar in magnitude but of opposite sign. During the time that each rod is in the channel, there is a 2% flow blockage that should have an insignificant effect on the axial velocity.

Repeat tests at the same operating condition at different days were performed to check for data uncertainty. Repeatability was good for all quantities except the radial velocity, which had fair repeatability. This is a difficult component to measure with the slant wire probe for the current geometry. Even for a 1000-record ensemble average, differences appeared between repeat tests for all velocity components. These differences are thought to be due to the randomness associated with vortex shedding from the gust generator rods. Measurements of individual instantaneous wakes show large variations (up to a factor of three) compared with the ensemble average.

#### Gust-Synchronized Surface Pressure

The compact interaction noise is controlled by the unsteady lift on the vane, which is composed of the integrated unsteady pressures on the vane. Gust-synchronized, ensemble-averaged surface pressure measurements were obtained at seven locations from 4.2 to 95.8% chord for the baseline, unactuated case. These are shown in Fig. 5. The instantaneous pressure  $p'$  is nondimensionalized by the dynamic pressure  $\frac{1}{2}\rho U^2$ . A nondimensionalized time is represented by

$$t' = \frac{tU}{b} \quad (2)$$

where  $t$  is the time, and  $U$  is the freestream velocity.

The wake/airfoil encounter produces a sharp, negative impulse in surface pressure. The impulse is strongest close to the leading edge and drops to 10% of its value at the 4.2% chord station by the 50% chord location. The pressure pulse is nearly nonexistent over the downstream half of the airfoil.

#### Experimental Flap Motion Response

The frequency response of the actuated flap system was measured by a computerized system. The flap was commanded to move in sinusoidal motions at a given frequency and the requested and actual positions of the system were recorded. A fast Fourier transform (FFT) of both positions was computed, and the amplitude and phase were compared. A normalized amplitude was determined by dividing the actual position amplitude by the commanded position amplitude. Likewise, a phase lag was determined. The process was then repeated for higher and higher frequencies. In this way, an automated Bode plot was obtained.

Using this system, it was determined that up to  $\pm 7$  deg of flap motion was achievable at frequencies up to 100 Hz. For flap amplitudes of 2 deg, the frequency could be pushed to 150–200 Hz. These higher frequency responses contained phase lags in excess of 100 deg. In general, the system response for various flap amplitudes was very nonlinear.

#### Nonactuated Flap Interaction Noise

To measure the dipole characteristic of the interaction noise, microphones were placed out of the flow, directly above and below the airfoil span. The signals from these two microphones were differenced to accentuate the acoustic dipole properties. However, the gust generator produced its own self-noise as the rods intersected the test section. It was necessary to remove this background noise from the measured signal so that only interaction noise would be left. Therefore, separate measurements of the gust generator self-noise with the vane removed were also acquired before each test condition run. This signal was subtracted from the composite noise signal consisting of the gust generator self-noise and rotor/stator interaction noise. The resulting acoustic signature will be referred to as the net dipole in the remaining discussion.

The clearest indication of the interaction noise signature is obtained by subtracting the gust self-noise dipole signal from the gust/airfoil dipole signal resulting in a net dipole signature. The gust self-noise dipole and the gust/airfoil dipole signals were obtained by differencing the signals from the microphones located above and below the vane. A schematic diagram indicating the process involved in producing the net interaction dipole noise is shown in Fig. 6. An example of the raw and processed microphone signals corresponding to Fig. 6 is shown in Fig. 7. The time base in this figure has been nondimensionalized following the notation of Fujita and Kovaszny.<sup>5</sup> Acoustic measurements of the net dipole in that paper are similar to those obtained in the present study, although their study had only a single, sharp impulse. The net interaction dipole shown in Fig. 7 has one large pulse followed by several smaller waves. The cause for these secondary waveforms has not been determined.

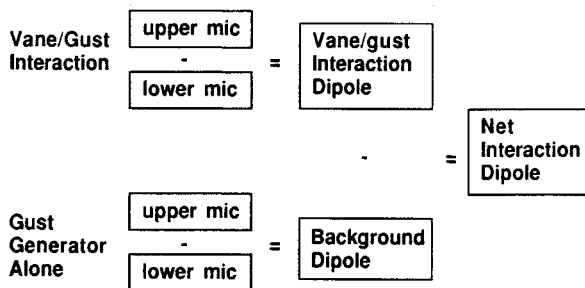


Fig. 6 Rotor/stator interaction noise data acquisition/processing procedure.

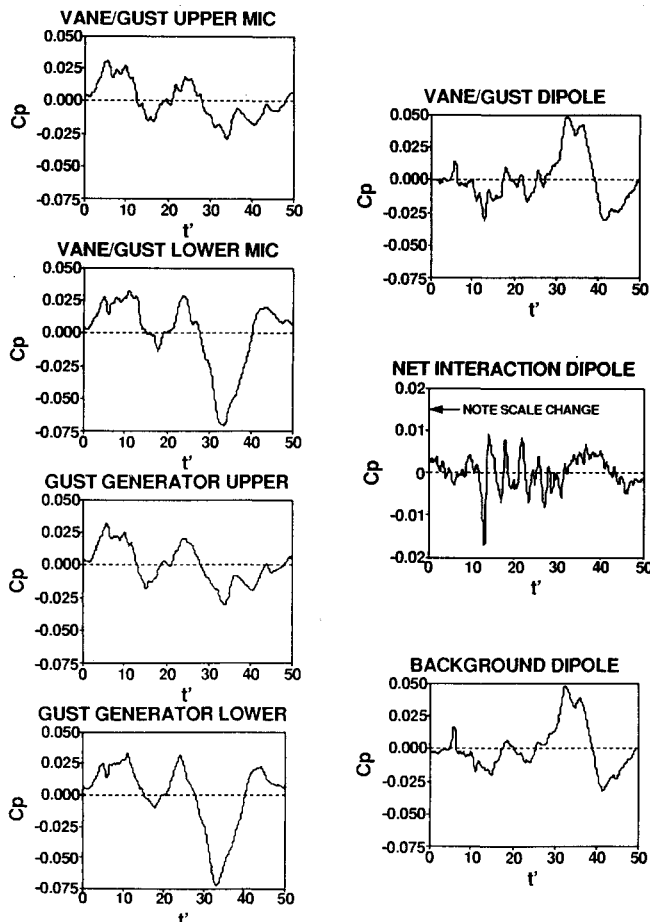


Fig. 7 Raw and processed rotor/stator interaction noise data.

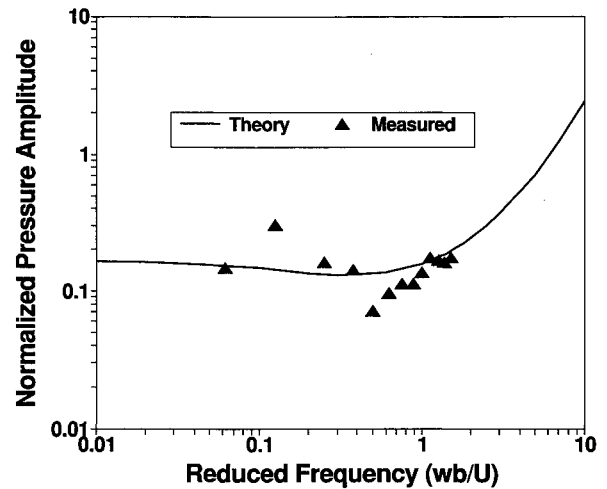


Fig. 8 Theoretical dipole noise prediction for sinusoidally oscillating trailing-edge flap, 5 deg amplitude.

#### Dipole Noise Measurement Confirmation

To give some confidence to the experimental technique, measurements of the noise generated by movement of the flap in a uniform stream were compared with acoustic dipole theory. By periodically moving the flap up and down on the actuated airfoil in a uniform stream (no gust generator), the lift distribution on the airfoil will change periodically. This in turn will generate noise that can be represented by a compact source. The dipole noise generated by the periodically oscillating flap can be measured and predicted with linearized unsteady airfoil theory. The flap was commanded to move in a sinusoidal motion with an amplitude of 5 deg. The resulting peak-to-peak acoustic pressure was obtained at flap frequencies ranging from 5 to 120 Hz (reduced frequencies of just below 0.1 to just over 1.0).

The corresponding theoretical airfoil lift was computed using the approach of Theodorsen. The unsteady (integrated) lift on the airfoil can be described by<sup>24</sup>

$$C_L(k) = -\frac{\pi}{U_0} \left[ C(k)(B_0 + B_1) - \frac{ik}{2} (B_1 - B_2) \right] e^{i\omega t} \quad (3)$$

where  $k = \omega b/U$  is the aerodynamic reduced frequency;  $C(k)$  is the Theodorsen function (which is a combination of Bessel functions); and  $B_0$ ,  $B_1$ , and  $B_2$  are the first three components of a Fourier series describing the airfoil upwash distribution along the airfoil.

With this unsteady lift prediction, the dipole noise can be computed, assuming the noise source is compact. At the low reduced frequencies studied here, this assumption is justified. The link between the lift change and dipole noise is then given by<sup>25</sup>

$$\frac{p}{\rho U^2} = \frac{i}{2} M C_L(k) H_1^{(1)} \left( k M \frac{r}{b} \right) \cos \theta \quad (4)$$

where  $H_1^{(1)}$  is Hankel function of the first kind, order one,  $r$  is the radial distance from the noise source, and  $\theta$  is the angle between airfoil normal and measurement location.

The measurements of flap dipole pressure (per radian of flap motion) over the measured frequency range are compared with theoretical predictions in Fig. 8. The pressure amplitude has been normalized by the dynamic pressure  $\frac{1}{2} \rho U^2$ . The agreement between the theory and the experiment is good, giving some confidence in the microphone differencing used to measure the dipole noise.

#### Actuated Flap Noise Reduction

From the principle of Fourier series, it is possible to show that any arbitrary function can be described by a series of sine

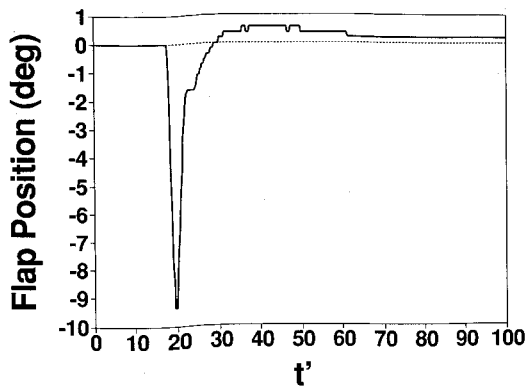


Fig. 9 Instantaneous flap position vs. time.

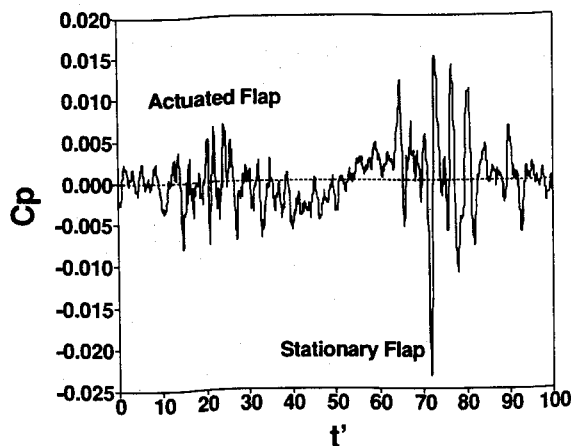


Fig. 10 Net dipole acoustic pressure trace with flap actuated on first rod wake and stationary on second rod wake.

waves. In principle, any of the individual harmonics of the interaction noise signature could be eliminated one by one by actuating the flap at the same frequency and at the correct amplitude and time delay or phase angle. However, the pressure trace of the net dipole signature in the far right of Fig. 7 shows an impulsive behavior. Such impulses are composed of a rich series of harmonics. It was, therefore, hypothesized that to eliminate the entire interactive net dipole it would be necessary to apply an impulsive unsteady flap motion that would generate a corresponding impulsive unsteady lift capable of countering the fluctuating vane lift.

The servomotor controller was, therefore, programmed to provide the most impulsive signal possible within the frequency response limits of the servomotor system. The delay time between the once-per-revolution signal and the start of flap actuation was varied manually to minimize the interaction noise. The actual flap motion that achieved the best noise reduction result is shown in Fig. 9 where the flap moved about 9 deg upward. The width of the pulse was about 8 ms. It is interesting to note that this flap profile (with a rapid rise and a slower recovery back to 0 deg) is very similar to that predicted theoretically by Kerschen<sup>22</sup> to cancel the incoming gust. The acoustic net dipole for this actuated case is shown in Fig. 10.

To demonstrate the benefit of the current active aerodynamic noise reduction concept, a direct comparison was made between the actuated and nonactuated interaction noise. The approach involved programming the flap to move for only one of the two rod passages that occurs each revolution. In this case, the flap was actuated for the first rod wake/vane interaction and held stationary at 0 deg for the second interaction. Figure 10 shows the net dipole pressure trace for an ensemble

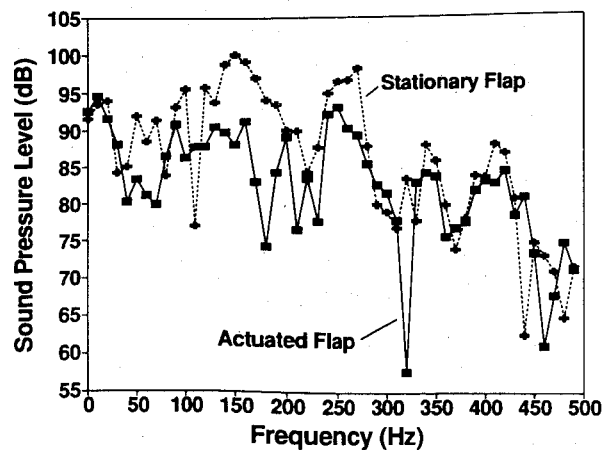


Fig. 11 Net dipole sound pressure level comparison of flap actuated and flap stationary.

average of 200 interactions. The peak-to-peak pressure is reduced by at least a factor of 2 when the flap is actuated. To visualize the frequency contributions for the actuated and nonactuated interactions, the signal in Fig. 10 was broken into two halves, and an FFT was performed on each half. This result is shown in Fig. 11. The dashed trace shows the nonactuated result, and the solid line shows the actuated result. Substantial reductions occur over portions of the spectrum. Reductions as high as 10 dB or more occur at some frequencies.

### Summary and Conclusions

A technique for interaction noise reduction using active aerodynamic control has been demonstrated for a simple system consisting of a two-bladed rotor and a single vane. This concept can be applied to more complex systems. A servo-actuated trailing-edge flap vane was used to counter the unsteady lift created by an incident gust, thereby reducing the unsteady surface pressure and hence interaction noise. The peak-to-peak acoustic dipole pressure was reduced by a factor of 2 and reductions of 10 dB or more occur over portions of the acoustic spectrum. Such dramatic results indicate that it is possible to attack unsteady loading noise at the aerodynamic source, which is an advantage since the noise reduction is global in extent.

### Acknowledgments

This program would not have been possible without the support of a number of talented individuals. Key in the planning and direction of the program were R. H. Schlinker, manager of Aeroacoustics and Experimental Gas Dynamics at UTRC, D. C. Mathews of Pratt and Whitney, D. B. Hanson of Hamilton Standard, and E. J. Kerschen of the University of Arizona. The servomotor logic control system was designed and implemented by D. P. Cornell.

### References

- <sup>1</sup>Tyler, J. M., and Sofrin, T. G., "Axial Flow Compressor Noise Studies," *Society of Automotive Engineers Transactions*, Vol. 70, 1962, pp. 309-332.
- <sup>2</sup>Sofrin, T. G., "Aircraft Turbomachinery Noise—Fan Noise," American Society of Mechanical Engineers/Iowa State Univ. Course in the Fluid Dynamics of Turbomachinery, Ames, IA, Lectures 21 and 22, July 1973, pp. 1-101.
- <sup>3</sup>Gallus, H. E., Grollius, H., and Lambertz, J., "The Influence of Blade Number Ratio and Blade Row Spacing on Axial-Flow Compressor Stator Blade Dynamic Load and Stage Sound Pressure Level," *Transactions of the ASME, Journal of Engineering for Power*, Vol. 104, No. 3, 1982, pp. 633-641.
- <sup>4</sup>Topol, D. A., "Rotor Wake/Stator Interaction Noise—Predictions Versus Data," AIAA Paper 90-3951, Oct. 1990.
- <sup>5</sup>Fujita, H., and Kovasznay, L. S. G., "Sound Generation by Wake

Cutting," AIAA Paper 73-1019, Oct. 1973.

<sup>6</sup>Fujita, H., and Kovaszny, L. S. G., "Unsteady Lift and Radiated Sound from a Wake Cutting Airfoil," *AIAA Journal*, Vol. 12, No. 9, 1974, pp. 1216-1221.

<sup>7</sup>Ho, C., and Kovaszny, L. S. G., "Wake Cutting by a Cascade of Cambered Blades," AIAA Paper 75-445, March 1975.

<sup>8</sup>Sugeng, F., and Fiedler, K., "An Experimental Investigation into Unsteady Blade Forces and Blade Losses in Axial Compressor Blade Cascade," *Transactions of the ASME, Journal of Engineering for Gas Turbines and Power*, Vol. 108, No. 1, 1986, pp. 47-52.

<sup>9</sup>Zandbergen, T., "Stator Vane Response Due to the Impingement of the Wake of an Unloaded Rotor," AIAA Paper 88-2814, July 1988.

<sup>10</sup>Lueg, P., "Process of Silencing Sound Oscillations," U.S. Patent No. 2,043,416, Dept. of Commerce, Patent and Trademark Office, Washington, DC, June 9, 1936.

<sup>11</sup>Ffowcs-Williams, J. E., "Anti-Sound," *Proceedings of the Royal Society of London, Series A*, Vol. 395, No. 1808, 1984, pp. 63-88.

<sup>12</sup>Stevens, J., and Ahuja, K. K., "The State-of-the-Art in Active Noise Control," AIAA Paper 90-3924, Oct. 1990.

<sup>13</sup>Ahuja, K. K., and Burrin, R. H., "Control of Flow Separation by Sound," AIAA Paper 84-2298, Oct. 1984.

<sup>14</sup>Salikuddin, M., Tanna, H. K., Burrin, R. H., and Carter, W. E., "Application of Active Noise Control to Model Propeller Noise," AIAA Paper 84-2344, Oct. 1984.

<sup>15</sup>Bullmore, A. J., Nelson, P. A., Elliott, S. J., Evers, J. F., and Chidley, B., "Models for Evaluating the Performance of Propeller Aircraft Active Noise Control Systems," AIAA Paper 87-2704, Oct. 1987.

<sup>16</sup>Salikuddin, M., and Ahuja, K. K., "Application of Localized Active Noise Control to Reduce Propeller Noise Transmitted Through Fuselage Surface," AIAA Paper 88-0266, Jan. 1988.

<sup>17</sup>Koopmann, G. H., and Fox, D. J., "Active Source Cancellation of the Blade Tone Fundamental and Harmonics in Centrifugal Fans," *Journal of Sound and Vibration*, Vol. 126, No. 2, 1988, pp. 209-220.

<sup>18</sup>Simpson, M., and Luong, T., "Full Scale Demonstration of Cabin Noise Reduction Using Active Vibration Control," AIAA Paper 89-1074, April 1989.

<sup>19</sup>Fuller, C., Snyder, S., and Hansen, C., "Active Control of Interior Noise in Model Aircraft Fuselages Using Piezoceramic Actuators," AIAA Paper 90-3922, Oct. 1990.

<sup>20</sup>Brooks, T. F., Booth, E. R., Jolly, J. R., Yeager, W. T., and Wilbur, M. L., "Reduction of Blade-Vortex Interaction Noise Through Higher Harmonic Pitch Control," *Journal of the American Helicopter Society*, Vol. 35, No. 1, 1990, pp. 86-91.

<sup>21</sup>Amiet, R. K., "High Frequency Thin-Airfoil Theory for Subsonic Flow," *AIAA Journal*, Vol. 14, No. 8, 1976, pp. 1076-1082.

<sup>22</sup>Kerschen, E. J., "Active Aerodynamic Control of Wake-Airfoil Interaction Noise—Theory," *Proceedings of the DGLR/AIAA 14th Aeroacoustics Conference*, Deutsche Gesellschaft für Luft- und Raumfahrt e. V., Bonn, Germany, May 1992, pp. 238-249.

<sup>23</sup>Lavrich, P. L., "Time Resolved Measurements of Rotating Stall in Axial Flow Compressors," Massachusetts Inst. of Technology, Gas Turbine Lab Rept. 194, Cambridge, MA, 1988.

<sup>24</sup>Robinson, A., and Laumann, J. A., *Wing Theory*, Cambridge Univ. Press, Cambridge, England, UK, 1956, pp. 481-526.

<sup>25</sup>Morse, P. M., and Ingard, K. U., *Theoretical Acoustics*, McGraw-Hill, New York, 1968, pp. 358, 359.

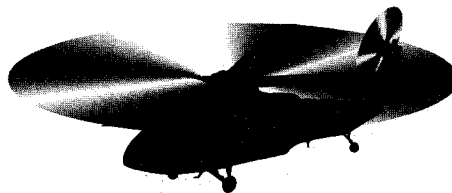
## Recommended Reading from the AIAA Education Series

# Basic Helicopter Aerodynamics

J. Seddon

*Basic Helicopter Aerodynamics* introduces the theory of rotary-wing aircraft for undergraduate and graduate students. The author explains the analytical treatment and solutions of helicopter theory so that the reader may fully understand the physical phenomena. Many diagrams, drawings, graphs, and representative sets of data augment the text.

All of the topics necessary for a complete understanding of single-rotor helicopter aerodynamics are included: basic physical concepts for the helicopter rotor in vertical and forward flight, including momentum theory and wake analysis; blade element theory; aerodynamic design; performance; trim; static and dynamic stability; control; and autostabilization.



1990 133 pp., illus. Hardback • ISBN 0-930403-67-3  
AIAA Members \$39.95 • Nonmembers \$49.95 • Order #: 67-3 (830)

Place your order today! Call 1-800/682-AIAA



American Institute of Aeronautics and Astronautics

Publications Customer Service, 9 Jay Gould Ct., P.O. Box 753, Waldorf, MD 20604  
FAX 301/843-0159 Phone 1-800/682-2422 9 a.m. - 5 p.m. Eastern

Sales Tax: CA residents, 8.25%; DC, 6%. For shipping and handling add \$4.75 for 1-4 books (call for rates for higher quantities). Orders under \$100.00 must be prepaid. Foreign orders must be prepaid and include a \$20.00 postal surcharge. Please allow 4 weeks for delivery. Prices are subject to change without notice. Returns will be accepted within 30 days. Non-U.S. residents are responsible for payment of any taxes required by their government.